

Basal Forebrain Cholinergic Neurons Have Specific Characteristics during the Perinatal Period

Natalia Lozovaya,¹ Anice Moumen,² and Constance Hammond¹

¹B&A Therapeutics, Marseille 13009, France and ²Neurochlore, Marseille 13009, France

Abstract

Cholinergic neurons of the basal forebrain represent the main source of cholinergic innervation of large parts of the neocortex and are involved in adults in the modulation of attention, memory, and arousal. During the first postnatal days, they play a crucial role in the development of cortical neurons and cortical cytoarchitecture. However, their characteristics, during this period have not been studied. To understand how they can fulfill this role, we investigated the morphological and electrophysiological maturation of cholinergic neurons of the substantia innominata–nucleus basalis of Meynert (SI/NBM) complex in the perinatal period in mice. We show that cholinergic neurons, whether or not they express gamma-aminobutyric acid (GABA) as a cotransmitter, are already functional at Embryonic Day 18. Until the end of the first postnatal week, they constitute a single population of neurons with a well developed dendritic tree, a spontaneous activity including bursting periods, and a short-latency response to depolarizations (early-firing). They are excited by both their GABAergic and glutamatergic afferents. During the second postnatal week, a second, less excitable, neuronal population emerges, with a longer delay response to depolarizations (late-firing), together with the hyperpolarizing action of GABA_A receptor-mediated currents. This classification into early-firing (40%) and late-firing (60%) neurons is again independent of the coexpression of GABAergic markers. These results strongly suggest that during the first postnatal week, the specific properties of developing SI/NBM cholinergic neurons allow them to spontaneously release acetylcholine (ACh), or ACh and GABA, into the developing cortex.

Key words: basal forebrain; cholinergic neurons; early-firing; late-firing; nucleus basalis Meynert; substantia innominata

Significance Statement

During early postnatal days, basal forebrain cholinergic neurons from the substantia innominata–nucleus basalis of Meynert (SI/NBM) complex play a crucial role in cortical development. However, their morphological and electrophysiological characteristics have not been studied during this period. Here we show that perinatal SI/NBM cholinergic neurons, whether they still express or have coexpressed GABAergic markers, belong to a single, homogeneous population of spontaneously active, early-firing, bursting neurons, activated by both glutamatergic and GABAergic afferents until the GABA_A receptor-mediated current polarity shift from excitatory to inhibitory has occurred. This early high excitability suggests that they can release acetylcholine (ACh) or ACh and GABA into the developing cortical layers and fulfill their well described role in the early development of cortical neurons and networks.

Introduction

Cholinergic neurons distributed within the basal forebrain (BF) nuclei, including the medial septum, the vertical and horizontal diagonal band of Broca, and the substantia innominata–nucleus basalis of Meynert (SI/NBM) complex, provide the main source of cholinergic innervation of the neocortex (Mesulam et al., 1983; Rye et al., 1984; Wu et

Received Nov. 13, 2023; revised April 9, 2024; accepted May 5, 2024.

C.H. and N.L. were employed by B&A Therapeutics, a startup dedicated to treat Parkinson's disease, at the time they performed the experiments, and A.M. was employed by Neurochlore, a startup dedicated to the development of treatments for children with autism. C.H. was a shareholder of B&A Therapeutics.

Author contributions: N.L. and C.H. designed research; N.L. and A.M. performed research; N.L. analyzed data; N.L. and C.H. wrote the paper.

We thank A. Dufour and A. Pons-Bennaceur for their technical support. We thank N. Burnashev and Y. Ben Ari for their helpful comments on previous versions of the manuscript and H. Rabiei for his comments on the reviewed version of the manuscript. This work was supported by Servier Pharmaceuticals, B&A Therapeutics, and Neurochlore.

Correspondence should be addressed to Natalia Lozovaya at lozovaya@ba-oncomedical.fr.

Copyright © 2024 Lozovaya et al. This is an open-access article distributed under the terms of the Creative Commons Attribution 4.0 International license, which permits unrestricted use, distribution and reproduction in any medium provided that the original work is properly attributed.

al., 2014; Zaborszky et al., 2015; Boskovic et al., 2019). They are implicated in the maintenance of the sleep–wake cycle and in the processes underlying arousal and attention modulation (Brown et al., 2012; Monosov et al., 2015; Ballinger et al., 2016; Zant et al., 2016). Adult BF cholinergic neurons exhibit heterogeneity based on molecular and electrophysiological features. A large subpopulation coexpresses the necessary cell machinery for GABA release, that is, the GABA synthetic enzyme, glutamate decarboxylase GAD65 (*Gad2*), and the vesicular GABA transporter (*Slc32a1*). Acetylcholine (ACh) and GABA are cotransmitters since optogenetic stimulation of cholinergic fibers evokes monosynaptic synaptic currents mediated by both nicotinic ACh (nAChRs) and GABA_A receptors (GABA_ARs) in Layer 1 cortical interneurons. The GABA_AR-mediated component disappears after selective conditional knock-out of *Slc32a1* in cholinergic neurons (Kosaka et al., 1988; Tkatch et al., 1998; Grill et al., 2004; Henny and Jones, 2008; Saunders et al., 2015; Granger et al., 2016; Case et al., 2017). Additionally, two distinct functional cholinergic cell types, the “early-firing” and “late-firing” neurons, are described in vitro and in vivo in adult mouse BF (Unal et al., 2012; Laszlovsky et al., 2020). In vivo, “early-firing” neurons are burst-firing neurons that can synchronize, whereas “late-firing” neurons are nonsynchronized regular firing neurons. They are likely to perform different roles in adult cortical activity and behavior (Laszlovsky et al., 2020). A possible correlation between the presence or absence of GABA as a cotransmitter and the two distinct functional populations has not been studied.

During early postnatal days, BF cholinergic neurons play a crucial role in cortical development. Growth cone-tipped choline acetyl transferase (ChAT)-positive axons are present in the subplate of frontal, parietal, and occipital cortices of rat pups from birth (P0) onward (Mechawar and Descarries, 2001). In the mouse pups, the density of acetylcholinesterase (AChE)-stained fibers increases significantly throughout the cortex from P0 to the second postnatal day (P2) and most of the AChE-positive fibers are located below the cortical plate, with some staining visible in the molecular layer (Höhm and Ebner, 1985). Between P4 and P16, the number of varicosities per micrometer of ChAT-immunostained axon increases sharply in all cortical areas and layers and stabilizes thereafter to reach adult values (see review in Bruehl-Jungerman et al., 2011). Moreover, functional muscarinic and calcium-permeable nAChRs are already present in the developing mouse cortex before birth (Atluri et al., 2001; Hohmann, 2003). Nonselective electrolytic or immunotoxic lesions of the NBM cholinergic region performed in rat pups at P0/P2 or specific lesion of NBM cholinergic neurons at P4 all result in delayed cortical neuronal development and permanently altered cortical cytoarchitecture and cognitive behaviors. This includes a reduced size of soma, dendritic abnormalities, altered connectivity, and synaptic plasticity (Hohmann et al., 1988; Hohmann and Berger-Sweeney, 1998; Robertson et al., 1998; Berger-Sweeney et al., 2001; Ricceri et al., 2002; Hohmann, 2003; Kuczewski et al., 2005). However, morphological and electrophysiological characteristics of BF cholinergic neurons have not been studied during this perinatal period.

To better understand why SI/NBM cholinergic neurons have such an impact on the development of cortical neurons and networks during the first postnatal days, we investigated their morphological and functional characteristics from Embryonic Day 18 (E18) to P15. We aimed at identifying the extent of their dendritic tree, their membrane properties, the impact of their afferent connections, and their type of ongoing activity. With the use of transgenic *Lhx6-iCre^{+/-}; RCE-EGFP^{+/-}* mice, we could separately record and label in the SI/NBM region, the two cholinergic populations, and the cholinergic/GABAergic (ChAT⁺ EGFP⁺) and cholinergic/non-GABAergic (ChAT⁺ EGFP⁻) neurons (Lozovaya et al., 2018).

Materials and Methods

Animals

We generated transgenic mice *Lhx6-iCre^{+/-};RCE-EGFP^{+/-}* by crossing *Lhx6-iCre^{+/-};RCE-EGFP^{+/-}* mice (a generous gift from Prof. Gordon J. Fishell) with wild-type Swiss mice (CE Janvier). Vaginal plugs were checked early the following morning at 7 A.M. and noted as E0.5 of gestation. Mice were maintained on a 12 h light cycle (7 A.M.–7 P.M.) with *ad libitum* access to food and water. Experiments were performed in both males and females, in agreement with the European Community Council Directives (2010/63/UE). Protocols were approved by the local French ethical committee for animal experimentation (19196) and validated by the French Ministry of Higher Education, Research and Innovation (authorization 19196-2018071214167976).

We used slices from *Lhx6-iCre^{+/-};RCE-EGFP^{+/-}* mice, because EGFP expression allowed characterizing GABA/ACh neurons after post hoc ChAT immunocytochemistry. EGFP expression also allowed delineating the border of the globus pallidus (GP) since all GP cells are EGFP⁺ and fluorescent. This was particularly important in very young animals.

Slice preparation and patch-clamp recordings. For prenatal date E18, we killed pregnant dams by cervical dislocation and rapidly (in 20–30 s) isolated uterine horns from their blood supply. We immediately delivered and decapitated pups. We removed fetuses from timed-pregnant females 24 ± 6 h before the estimated day of delivery. For postnatal dates P0–P5, we quickly killed pups by decapitation, but after P5 we anesthetized pups with isoflurane before decapitation. We kept brains in ice-cold oxygenated solution containing the following (in mM), 118 choline chloride, 2.5 KCl, 0.7 CaCl₂, 7 MgCl₂, 1.2 NaH₂PO₄, 26 NaHCO₃, and 8 glucose, and performed parasagittal slices (300–350 μm thick) using a vibratome (VT1200 Leica Microsystems). During the recovery period (at least 2 h), slices were placed at room temperature (RT, 22–25°C) in standard artificial cerebrospinal fluid (ACSF) saturated with 95% O₂/5% CO₂ and containing the

following (in mM): 125 NaCl, 3.5 KCl, 0.5 CaCl₂, 3 MgCl₂, 1.25 NaH₂PO₄, 26 NaHCO₃, and 10 glucose, 300 mOsm⁻¹. For recordings, we used an ACSF of the same composition but containing 2 mM CaCl₂ and 1 mM MgCl₂. Slices were transferred to the recording chamber and perfused with oxygenated ACSF (3 ml/min) at RT. Neurons were visualized using infrared-differential interference optics (Microscope Olympus BX51WI). Patch pipettes were pulled from borosilicate glass capillaries (World Precision Instruments). In parasagittal slices from Lhx6-iCre;RCE-EGFP mice, we identified the dual cholinergic/GABAergic neurons as EGFP⁺ neurons and the cholinergic neurons as EGFP⁻ neurons with a large soma (≥ 40 μ m diameter), thick primary dendrites, and a typical response to hyperpolarizing pulses. Their cholinergic nature was later confirmed with post hoc immunocytochemistry (see below, Immunohistochemistry, reconstruction of biocytin-filled neurons, and Sholl analysis). We performed cell-attached recordings 5–7 min after establishment of the gigaohm seal and after stabilization of the baseline with patch pipettes filled with extracellular solution. For whole-cell recordings, patch pipettes (World Precision Instruments) were filled with intracellular solution as follows (in mM): 130 K-gluconate, 10 Na-gluconate, 7 NaCl, 4 MgATP, 4 Na₂-phosphocreatine, 10 HEPES, and 0.3 GTP, pH 7.3 (with KOH, 280 mOsm⁻¹), and biocytin (final concentration of 0.3–0.5%). In whole-cell recordings, equilibrium potential for chloride ions was around –75 mV and equilibrium potential for AMPA channels ~0–10 mV. We discarded cells with leakage current over 40–50 pA. Whole-cell recordings were performed with the EPC-10 amplifier and PATCHMASTER software v2 x 73.2 (HEKA Elektronik) and filtered at 3–10 kHz. To determine current–voltage (I–V) relationships and calculate input resistance of cells, we recorded voltage responses (current-clamp mode) to a series of 1 s current pulses. For the hyperpolarization-activated sag parameters, we measured the ratio between the peak amplitude and the amplitude at the end of the voltage response. We measured the half-width duration of action potentials (APs) at half the amplitude between the AP peak and threshold potentials. We measured the after-hyperpolarization (AHP) amplitude between AP threshold potentials and AHP peak. The Clampfit 10.6.2.2 (Molecular Devices), Igor 6.3.7.2 (WaveMetrics), and OriginPro software were used for analysis. Spontaneous postsynaptic outward currents were recorded at $V_H = 0$ to +10 mV closest to the reversal potential of AMPA receptor-mediated currents, and spontaneous postsynaptic inward currents were recorded at –70 mV, close to the reversal equilibrium potential of chloride ions.

Immunohistochemistry, reconstruction of biocytin-filled neurons, and Sholl analysis. Parasagittal slices were incubated with ChAT primary antibody coupled with a donkey anti-goat Alexa Fluor 633 (1:500, The Jackson Laboratories). After 20–24 h fixation in 4% paraformaldehyde (Alfa Aesar, Thermo Fisher Scientific) in phosphate-buffered saline (PBS; Invitrogen, Thermo Fisher Scientific) at 4°C, slices were washed three times in PBS, and after a 1 h preincubation in PBS containing 10% normal donkey serum (NDS; Jackson ImmunoResearch Laboratories), 1% bovine serum albumin (BSA; Sigma-Aldrich, Merck KGaA), and 0.3% Triton X-100 (Sigma-Aldrich, Merck KGaA), they were incubated overnight at 4°C with goat anti-ChAT antibody (AB144P, Chemicon, Merck KGaA; 1:300) in PBS containing 1% NDS, 1% BSA, and 0.3% Triton X-100. Twenty-four hours after, slices were washed three times in PBS and incubated in PBS containing 1% BSA with a donkey anti-goat coupled to Alexa Fluor 555 (A-21432, Invitrogen, Thermo Fisher Scientific; 1:500) and streptavidin coupled to Alexa Fluor 647 (S32357, Invitrogen, Thermo Fisher Scientific; 1:500). Slices were then washed three times in PBS and coverslipped using a Fluoromount-G mounting medium (Invitrogen, Thermo Fisher Scientific). We followed a similar procedure to perform Lhx6 staining. We used a mouse anti-Lhx6 (1:50,000, Santa Cruz Biotechnology, ref. sc-271433) and a donkey anti-mouse antibody coupled to Alexa Fluor 647 (1:500, Invitrogen). For biocytin-filled cell localization, identification, and reconstruction, confocal images were acquired on a SP8X Leica microscope (Leica Microsystems) using a diode 405 for the excitation of Hoechst or Alexa Fluor 405 (5%, spectral detection 415–460 nm), an OPSP 488 for the excitation of EGFP or Alexa Fluor 488 (10%, spectral detection 498–528 nm), an OPSP 552 for the excitation of Alexa Fluor 555 (5%, spectral detection 559–600 nm), and a diode 638 for the excitation of Alexa Fluor 647 (0.1%, spectral detection 649–776 nm). Images were acquired at 200 Hz using a 10 \times objective (for cells localization; pixel size, 2.2705 μ m) and a 40 \times oil immersion objective (for cell identification and reconstruction; pixel size, 0.2838135 μ m), pinhole set to “Airy 1,” by scanning with a z step of 0.5016 μ m when needed. Images were edited using Photoshop and Illustrator (Adobe Systems Software Ireland). After image acquisition, stacks were imported in the open-source platform Fiji (<https://fiji.sc/>) and processed for neuron reconstruction and Sholl analysis (Lozovaya et al., 2018).

To confirm the cholinergic identity of the recorded neurons, we revealed the biocytin injected during whole-cell recordings and performed post hoc ChAT immunohistochemistry. Recorded (biocytin-positive) neurons that were EGFP positive (EGFP⁺) and ChAT positive (ChAT⁺) were cholinergic neurons that have expressed (Lhx6⁻) or still express (Lhx6⁺) the LIM homeodomain 6 (Lhx6; Fig. 1A–C). Biocytin-positive neurons that were EGFP negative (EGFP⁻) and ChAT⁺ were cholinergic neurons that have never expressed Lhx6 (Lhx6⁻; Fig. 1A–C). The starting date of our study was E18 since it was the earliest date for optimal reliability of ChAT immunostaining (Fig. 1C).

Drugs

2,3-Dioxo-6-nitro-1,2,3,4-tetrahydrobenzo[*f*]quinoxaline-7-sulfonamide (10 μ M, Tocris Bioscience, Ref. 0373), isoguvacine (10 μ M, Sigma-Aldrich, Ref. G002), DL-2-Amino-5-phosphonovaleric acid (40 μ M, Sigma-Aldrich, Ref. A5282), picrotoxin (50 μ M, Tocris Bioscience, Ref. 1128), bumetanide (10 μ M, Sigma-Aldrich, Ref. B3023).

Statistical analysis and cluster analysis

Data from morphological and electrophysiological experiments were computed in Prism 8 (GraphPad Software) or OriginPro 019 (64-bit) 9.6.0.172 (OriginLab). They were tested for normality and homoscedasticity using the Shapiro–Wilk and Leven’s tests before performing statistical analysis. We analyzed morphological and electrophysiological data using a two-tailed *t* test or Mann–Whitney test. For multiple comparisons we used one-way ANOVA test followed by Fisher’s LSD post hoc test or one-way ANOVA/Kruskal–Wallis test followed by Dunn’s multiple-comparison post hoc test. We calculated means by averaging data from *n* cells. We also indicated the number of animals *N* for each dataset in the figure legends. We performed confidence interval estimation (95%) and effect size using Estimation Stats (<https://www.estimationstats.com/>; Claridge-Chang and Assam, 2016; Ho et al., 2019) and statistical power analysis using OriginPro (OriginLab) and Anasstats (Anasstats, www.anasstats.fr). All data are presented as means ± SEM (**p* < 0.05; ***p* < 0.01; ****p* < 0.001). We rejected null hypothesis when *P* was inferior to 0.05 and 95% CI did not contain zero. All data are included in Extended Data Tables 2-1, 3-1, 4-1, 5-1, 6-1, and 7-1. Data availability statement: all relevant data are available from the corresponding authors upon reasonable request.

For cluster analysis, we performed hierarchical clustering, *k*-means and principal component analysis (PCA) with Origin (OriginLab). We first performed hierarchical clustering using Euclidian distance metrics and group average searching to group neuronal populations. The electrophysiological parameters tested for this analysis were input resistance, delay of the first spike in response to juxtathreshold depolarization, amplitude and half-width of evoked AP, AP maximal frequency, V_{Thresh} , AHP amplitude, and sag amplitude in response to –50 and –100 pA. We then performed a PCA to identify the correlation between the different analyzed features and applied the screen plot “elbow” criterion to determine the number of clusters. To detect and characterize the subpopulation of EGFP⁺ and EGFP[–] cholinergic cells, we performed *k*-means clustering based on selected parameters. *K*-Means silhouette indexes, specialized for measurement cluster quality (goodness), were calculated with Orange Data Mining Toolbox in Python (Demsar et al., 2014) to assess the cluster quality and validate the consistency within the cluster of data. The statistics of each cluster were used to characterize subpopulations and determine their phenotype, later named Clusters 1 and 2. We then compared results obtained with the two methods.

Results

Using Lhx6-iCre;RCE-EGFP mice (E18–P15) and post hoc ChAT immunohistochemistry, we identified ChAT⁺ EGFP⁺ and ChAT⁺ EGFP[–] neurons in the SI/NBM region (Fig. 1A–C; Extended Data Fig. 2-2A). We recorded 182 ChAT⁺ EGFP⁺ and 78 ChAT⁺ EGFP[–] cholinergic neurons in the SI/NBM region from 79 Lhx6-iCre;RCE-EGFP mice. Throughout the text, cholinergic/GABAergic neurons are ChAT⁺ EGFP⁺ neurons previously shown to coexpress GABAergic markers (Lozovaya et al., 2018), whereas cholinergic/non-GABAergic neurons are ChAT⁺ EGFP[–] neurons. We mainly focused the present study on ChAT⁺ EGFP⁺ neurons and compared some of their characteristics to ChAT⁺ EGFP[–] neurons.

Cholinergic/GABAergic neurons constitute a single population which rapidly develop during the first postnatal week

Figure 1D illustrates the typical perinatal development of dendritic trees of cholinergic/GABAergic neurons. Sholl analysis of the density profiles of dendritic branches of 3D-reconstructed, biocytin-filled, cholinergic/GABAergic neurons, as a function of distance from the soma (Fig. 2A,B), showed the initial exponential increase of all parameters (except critical value, i.e., the maximal number of dendritic intersections) from E18 to P2/3 or P4/5. Then, the area under the curve, total dendritic length, critical value, and number of dendritic nodes exponentially decreased from P2/3 to P8/9 before increasing again or stabilizing (Fig. 2B–H; Extended Data Table 2-1). These synchronous decreases probably reflected dendritic pruning (see Discussion). We did not detect significant change in the number of primary dendrites from E18 (4.7 ± 0.7 ; *n* = 15) to P14/15 [3.6 ± 0.3 (*n* = 16), *p* = 0.17].

In response to depolarizing steps, cholinergic/GABAergic neurons generated spikes at E18 (*n* = 13 out of 13) with a mean maximal frequency of 9.5 ± 1.9 Hz (*n* = 13; Fig. 3A,B). Maximal spike frequency and spike parameters (threshold potential, peak amplitude, half-width, after spike hyperpolarization maximal amplitude), together with membrane resistance and the amplitude of the depolarizing “sag” displayed back toward the baseline during a hyperpolarizing current pulse, all exponentially increased or decreased to peak values during the first postnatal days (from E18 to P3/P7; Fig. 3B–I; Extended Data Table 3-1).

We next wanted to test whether cholinergic/GABAergic neurons constituted two functional populations during the early postnatal period as described in the adult (Unal et al., 2012; Laszlovszky et al., 2020). We performed hierarchical and *k*-means cluster analyses based on the electrophysiological parameters (see Materials and Methods). This revealed that 96% of P2/5 cholinergic/GABAergic neurons belonged to a single population of neurons mostly characterized by a short delay of the first spike to juxtathreshold depolarization, the “early-firing” neurons (Fig. 4A,B,F–J; Extended Data Table 4-1), in contrast to the P12/15 neuronal population (see below). Therefore, SI/NBM cholinergic/GABAergic neurons constitute a single population of early-firing neurons at P2–5.

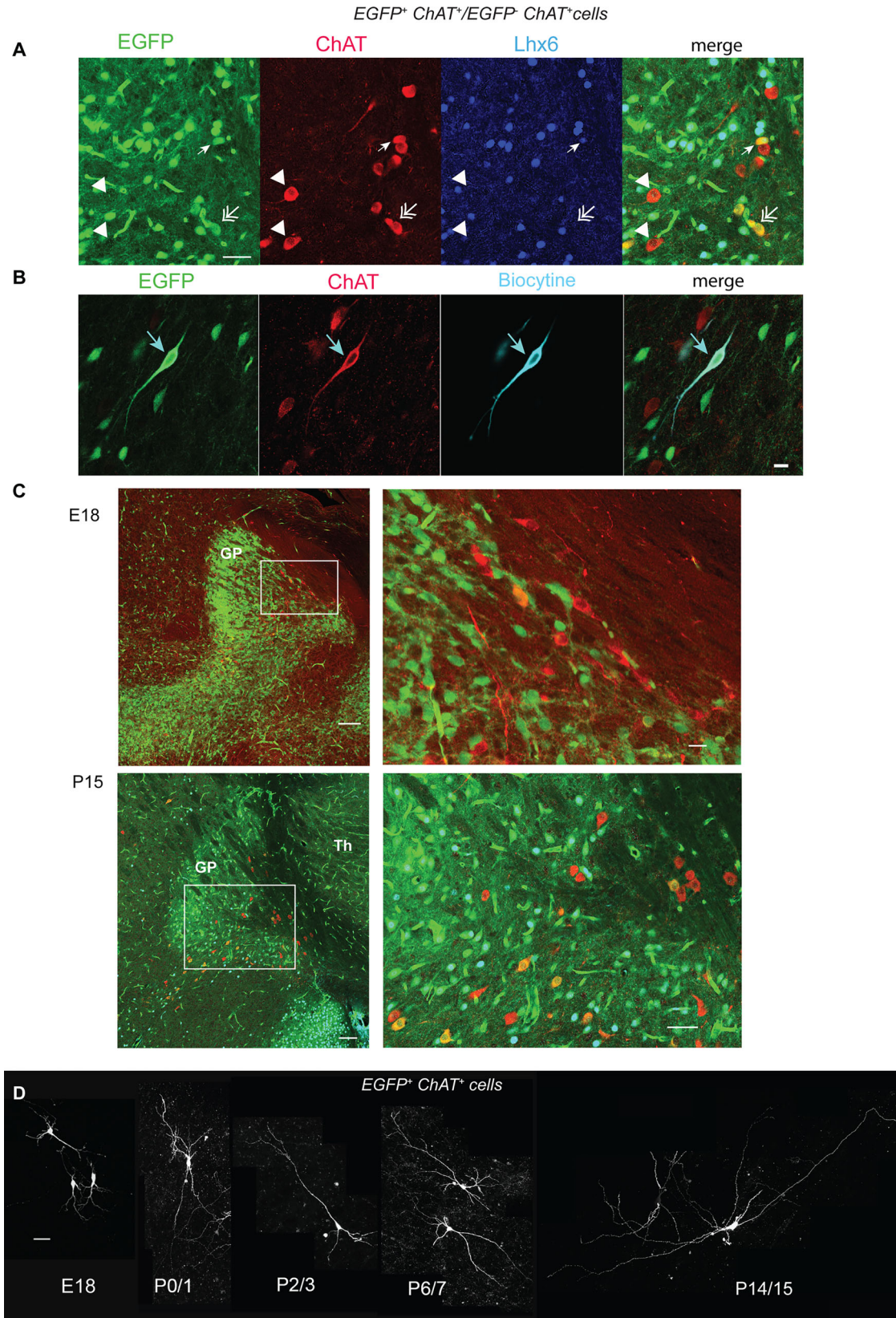


Figure 1. A subset of NBM cholinergic neurons expresses cholinergic (ChAT) and GABAergic (EGFP, Lhx6) markers in sagittal slices from Lhx6-iCre; RCE-EGFP mice. **A**, ChAT (red) and Lhx6 (blue) coimmunolabeling of a NBM neuron expressing EGFP (EGFP⁺, green, arrow). The double arrow points to an EGFP⁺ ChAT⁺ Lhx6⁻ neuron, and the two arrow heads point down to two EGFP⁻ ChAT⁺ Lhx6⁻ neurons of the same region. **B**, Example of EGFP

Cholinergic/non-GABAergic neurons also constitute a single population

Typical examples of reconstructed cholinergic/non-GABAergic (double arrow) and cholinergic/GABAergic (arrows) neurons at P5 are shown in Extended Data Fig. 2-2B. Statistical analysis of Sholl parameters did not reveal significant differences of dendritic tree parameters at P0/1 between cholinergic/GABAergic and cholinergic/non-GABAergic cells (but this could be due to the sample size), but later, at P4/5, cholinergic/non-GABAergic cells developed somewhat differently (Extended Data Fig. 2-2C-K; Extended Data Table 2-1). The great majority of electrophysiological parameters were similar at P0/1 and at P4/5 (Extended Data Fig. 3-2; Extended Data Table 3-1). Using the same parameters for hierarchical cluster analysis (Fig. 4), we showed that P2/5 cholinergic/non-GABAergic neurons (EGFP⁻) also constituted a single population of early-firing neurons (Extended Data Fig. 4-2A,F-J). We did not observe significant differences of the parameters tested (maximal frequency of evoked spikes, delay of the first spike in response to juxtathreshold depolarization, and AHP maximal amplitude) between cholinergic/GABAergic and cholinergic/non-GABAergic cells (Extended Data Fig. 4-2B,F-H; Extended Data Table 4-1). These results show that cholinergic/GABAergic and cholinergic/non-GABAergic neurons were both present at E18 in the SI/NBM region and constituted a single population of early-firing neurons throughout the first postnatal days (P2/5). Since ChAT⁺ EGFP⁺ and ChAT⁺ EGFP⁻ neurons shared similar electrophysiological characteristics, we extended our investigations to ChAT⁺ EGFP⁺ neurons only.

Activation of GABA_ARs excites cholinergic/GABAergic neurons during the first postnatal week

To test the polarity of the GABA_AR-mediated response of cholinergic/GABAergic neurons during the first postnatal week, we recorded the effects of the GABA_AR agonist isoguvacine on their spontaneous activity in noninvasive, cell-attached, patch-clamp recordings. From P2 to P7, focal application of isoguvacine increased the frequency of ongoing spike activity to 2.65 times ($n = 9$; $p = 0.003$) at P2/3, to 2.52 times ($n = 12$; $p = 0.001$) at P4/5, and to 1.77 times ($n = 16$; $p = 5 \times 10^{-5}$) at P6/7 that of control (Fig. 5; Extended Data Table 5-1). In 4 out of 10 cells, we observed a dual excitatory-inhibitory effect of isoguvacine in some of the recordings, the inhibitory part resulting from the shunting effect of isoguvacine as described by Branchereau and colleagues (Branchereau et al., 2016). These results suggest that activation of GABA_AR by afferent GABAergic synapses depolarize and activate postsynaptic cholinergic/GABAergic neurons throughout the first postnatal week.

Cholinergic/GABAergic neurons are spontaneously active and generate GABA_AR- and AMPAR-mediated currents already at birth

Spontaneous postsynaptic outward currents ($V_H = +10$ mV), sensitive to picrotoxin (50 μ M), were already present at birth. These GABA_AR-mediated PSCs had a mean amplitude of 60.0 ± 8.7 pA and a mean frequency of 1.0 ± 0.3 Hz at P0/1 ($n = 7$; Fig. 6; Extended Data Table 6-1). Spontaneous postsynaptic inward currents ($V_H = -70$ mV) sensitive to CNQX (10 μ M) were also already present at birth. These AMPAR-mediated PSCs had a mean amplitude of 5.4 ± 1.5 pA and a mean frequency of 1.2 ± 0.3 Hz at P0 ($n = 9$; Fig. 7; Extended Data Table 7-1). The frequencies of these spontaneous postsynaptic outward and inward currents significantly increased during the first postnatal week.

These results show that GABA_A and AMPA synapses afferent to cholinergic/GABAergic neurons were present and spontaneously active already at birth. Until GABA polarity shift occurred, both GABA_AR- and AMPAR-mediated PSCs had a depolarizing action (Fig. 5). This suggests that during the first postnatal week, both GABAergic and glutamatergic afferents excite cholinergic/GABAergic neurons which are all of the early-firing type (Fig. 4A,B; Extended Data Fig. 4-2A,B). These excitations should sustain their spontaneous activity. Noninvasive cell-attached recordings (so as not to change the intracellular concentration of chloride ions) revealed that cholinergic/GABAergic neurons were spontaneously active already at birth with a mean frequency of 3.15 ± 0.07 Hz ($n = 800$ events, seven cells). The pattern of activity was irregular with bursting periods up to P6/7, as attested by the presence of frequencies up to 15 Hz and over (Fig. 8).

During the second postnatal week GABA becomes inhibitory and cholinergic neurons separate into two populations endowed with different electrical properties

We then studied how GABAergic and non-GABAergic cholinergic neurons developed in parallel with GABA polarity shift. During the second postnatal week, three of the morphological parameters studied exponentially increased after their transient decrease (area under the curve, total dendritic length, and critical value). For all the other parameters, we did not observe significant changes after P4/5 (but this could be due to the sample size; Fig. 2C-H; Extended Data Table 2-1). When comparing morphological parameters of cholinergic/GABAergic neurons with cholinergic/non-GABAergic neurons, we did not observe significant differences at P14/15, despite the somewhat different development of some of the parameters of cholinergic/non-GABAergic neurons (Extended Data Fig. 2-2C-K; Extended Data Table 2-1). Similarly, we did not

←
expression (green) and ChAT staining (red) in a biocytin-filled (blue) neuron (arrow). **C**, EGFP expression (green) and ChAT staining (red) in a subset of NBM neurons at E18 and P15. On the right are the enlargements of the NBM region as indicated on the left. **D**, Representative biocytin-filled cholinergic/GABAergic (EGFP⁺ ChAT⁺) neurons at the indicated ages. Scale bars: **A**, 50 μ m; **B**, 50 μ m; **C**, E18, 100 μ m, 20 μ m; P15, 200 μ m, 100 μ m; **D**, 50 μ m.

EGFP⁺ ChAT⁺ cells

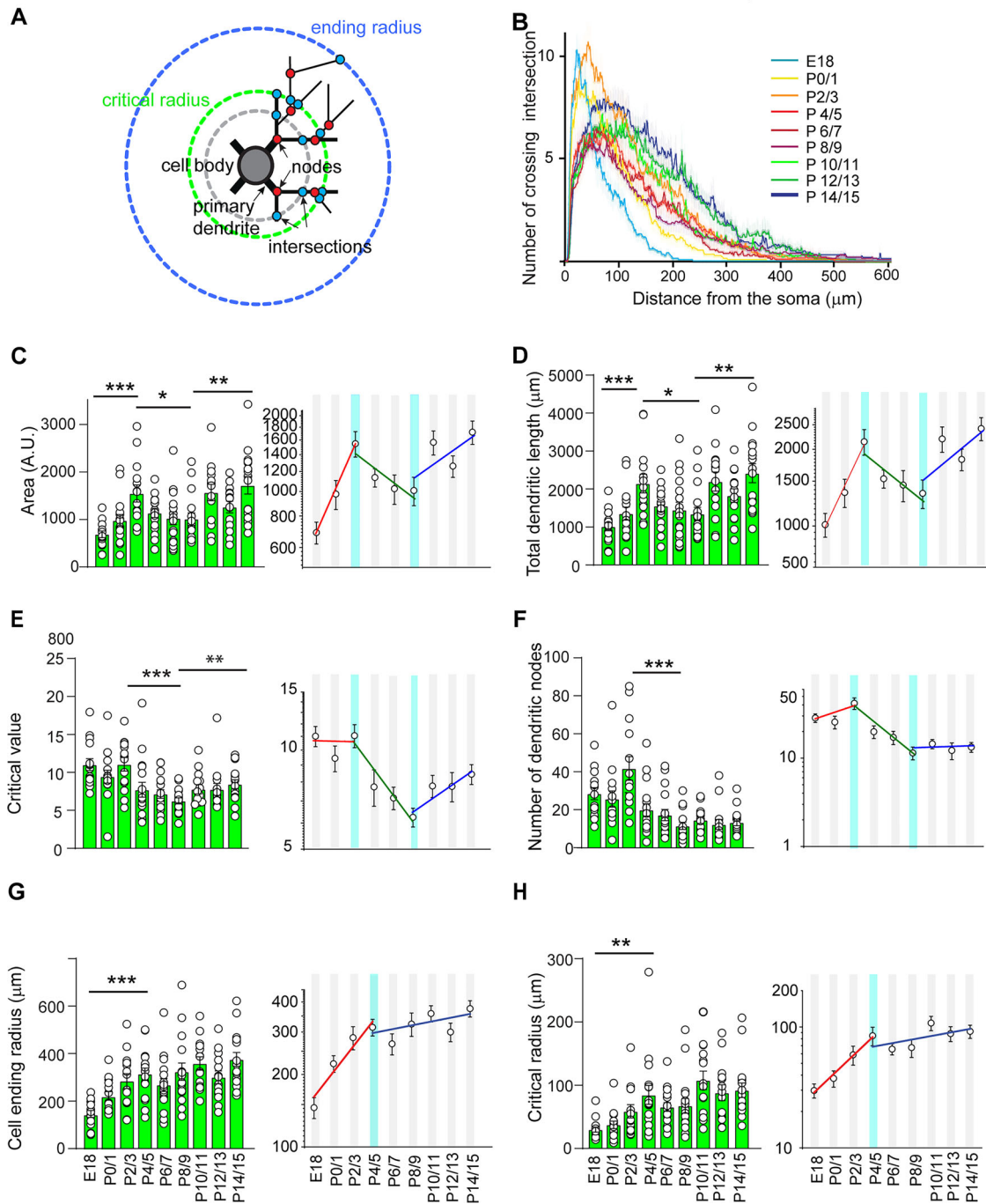


Figure 2. Development of the morphological properties of cholinergic/GABAergic neurons (E18–P15). **A**, Schematic representation of the quantified morphological parameters; the Sholl profiles (**B**) and morphological parameters (**C–H**) were obtained by overlaying a template of concentric and equidistant circles onto a two-dimensional images of biocytin-filled neurons with the first circle centered on the soma (radius 0); nodes (red dots), the points of branching of dendrites; crossing intersections (blue dots), the points where the dendritic branches intersect the Sholl circles; critical radius (green), the radius of the circle with the maximum number of crossing intersections; critical value, the number of crossing intersections at critical radius; ending radius (blue), the maximal radius of the circle with crossing intersection(s); the Sholl profile is the number of crossing intersections as a function of the radial distance from the cell soma. **B**, Mean Sholl profiles at the indicated ages. **C–H**, Left, Quantification of the main morphological properties (as indicated in ordinates) during development (abscissae). **C–H**, Right, Linear fits of fast (red) changes of the same morphological parameters in semilog Y coordinates. The light blue vertical bar indicates the peaks of development. E18: $n = 15$, $N = 4$; P0/1: $n = 15$, $N = 7$; P2/3: $n = 14$, $N = 6$; P4/5: $n = 17$, $N = 6$; P6/7: $n = 17$, $N = 6$; P8/9: $n = 16$, $N = 5$; P10/11: $n = 14$, $N = 6$; P12/13: $n = 14$, $N = 6$; P14/15: $n = 16$, $N = 7$. n , number of cells; N , number of mice. Mean \pm SEM, * $p < 0.05$; ** $p < 0.01$; *** $p < 0.001$ (Extended Data Table 2-1). Comparison of the dendritic parameters of GABAergic and non-GABAergic cholinergic neurons is presented in Extended Data Figure 2-2.

EGFP⁺ ChAT⁺ cells

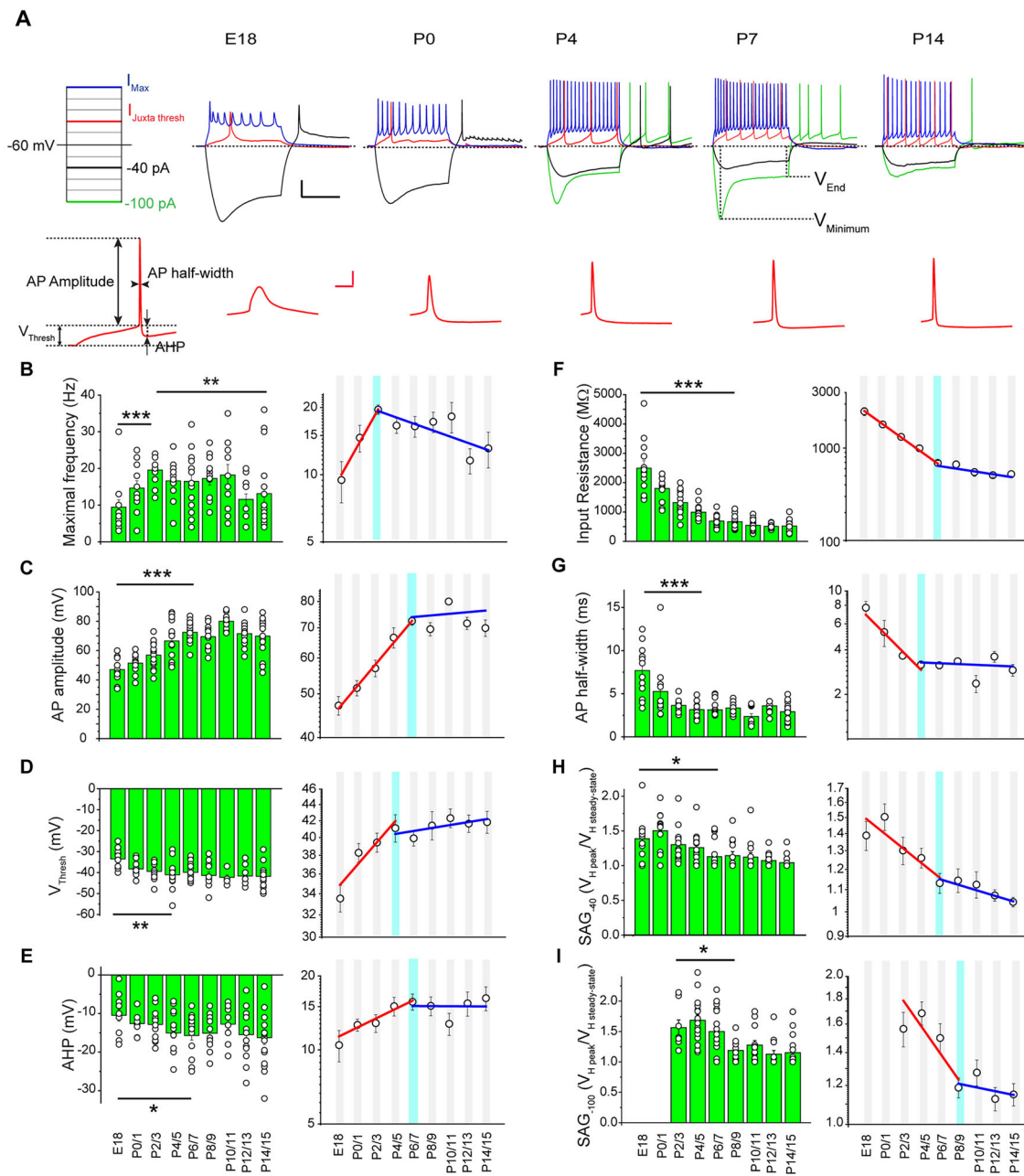


Figure 3. Development of the electrophysiological properties of cholinergic/GABAergic neurons (E18–P15). **A**, Top, Representative voltage responses to a series of current pulses (whole-cell configuration). Current injection protocol (left) depicts the pulses used to obtain the traces on the right. Sag amplitude was measured in response to hyperpolarizing pulses of -40 pA (black, SAG₄₀) or of -100 pA (green, SAG₁₀₀) as the ratio of amplitude between $V_{minimum}$ and V_{end} ; spike responses are displayed in response to juxtathreshold depolarizing (red) and maximal depolarizing (blue) current pulses. Bottom, Action potentials recorded in response to juxtathreshold depolarizing pulses at extended timescale (right) and the AP parameters measured (left). **B–I**, Left columns, Quantification of the main intrinsic membrane properties (as indicated in ordinates) during development (abscissae). **B–I** Right, Linear fits of fast (red) changes of the electrophysiological parameters in semilog Y coordinates. The light blue vertical bar indicates the peak of fast development. **B**, Mean maximal frequency. **C**, Mean AP amplitude. **D**, Mean AP threshold (V_{Thresh}). **E**, Mean AHP amplitude. **F**, Mean input resistance. **G**, Mean half-width of evoked APs. (E18: $n = 13$, $N = 4$; P0/1: $n = 11$, $N = 4$; P2/3: $n = 14$, $N = 6$; P4/5: $n = 15$, $N = 7$; P6/7: $n = 19$, $N = 7$; P8/9: $n = 12$, $N = 4$; P10/11: $n = 13$, $N = 4$; P12/13: $n = 14$, $N = 3$; P14/15: $n = 17$, $N = 6$). **H**, Mean sag amplitude in response to a -40 pA hyperpolarizing pulse (Sag₄₀; E18: $n = 12$, $N = 4$; P0/1: $n = 11$, $N = 4$; P2/3: $n = 12$, $N = 6$; P4/5: $n = 16$, $N = 8$; P6/7: $n = 18$, $N = 7$; P8/9: $n = 13$, $N = 5$; P10/11: $n = 13$, $N = 4$; P12/13: $n = 14$, $N = 3$; P14/15: $n = 17$, $N = 6$). **I**, Mean sag amplitude in response to a -100 pA hyperpolarizing pulse (Sag₁₀₀; P2/3: $n = 8$, $N = 6$; P4/5: $n = 16$, $N = 8$; P6/7: $n = 15$, $N = 7$; P8/9: $n = 13$, $N = 5$; P10/11: $n = 13$, $N = 4$; P12/13: $n = 13$, $N = 3$; P14/15: $n = 17$, $N = 6$). n , number of cells; N , number of mice. Mean \pm SEM, * $p < 0.05$; ** $p < 0.01$; *** $p < 0.001$ (Extended Data Table 3-1). Comparison of the intrinsic electrophysiological properties of GABAergic and non-GABAergic cholinergic neurons is presented in Extended Data Figure 3-2.

EGFP⁺ ChAT⁺ cells

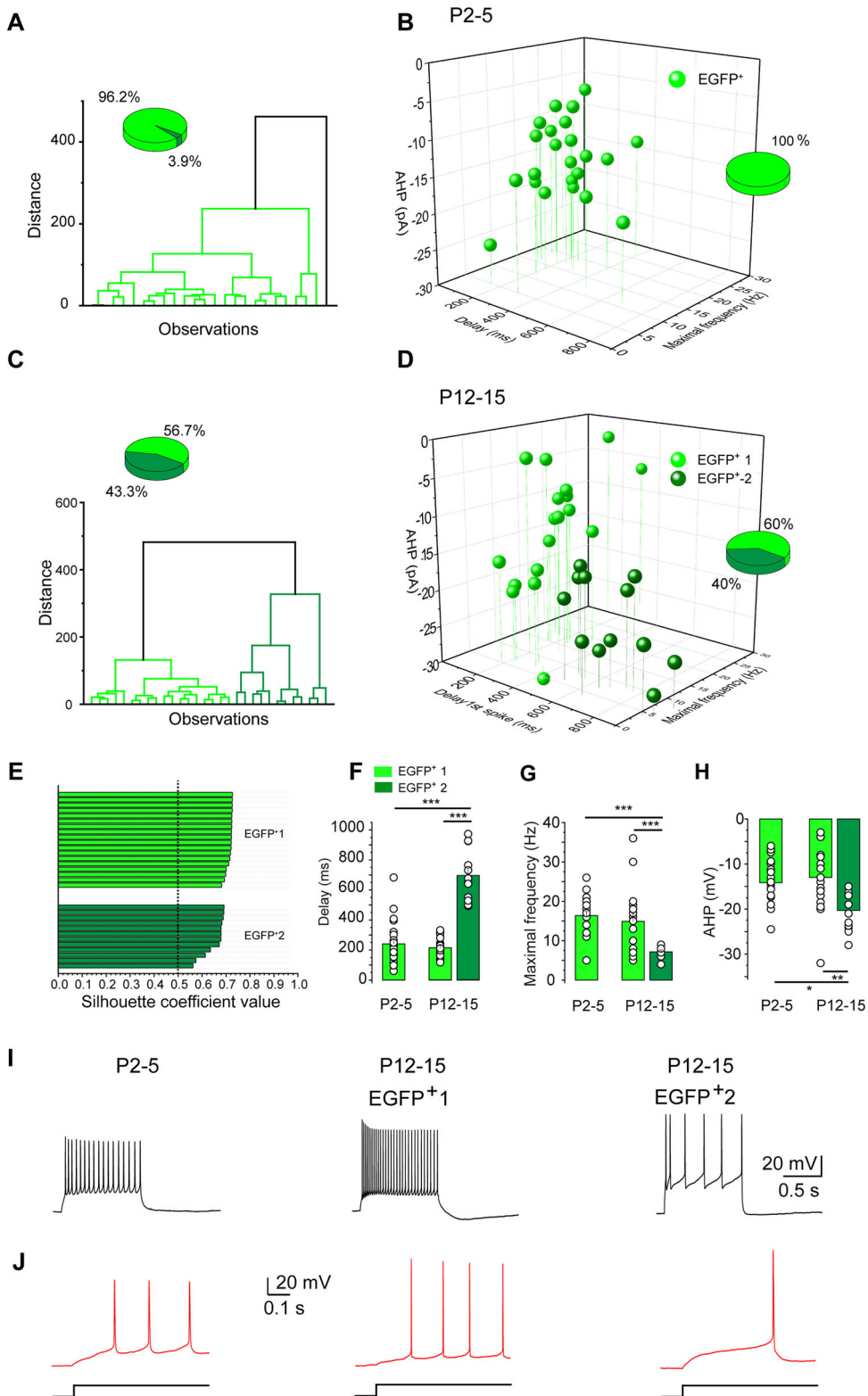


Figure 4. Cluster analysis of cholinergic/GABAergic neurons based on intrinsic electrophysiological properties at P2–5 and P12–15. **A**, Hierarchical clustering dendrogram for intrinsic electrophysiological properties of P2–5 neurons (delay of the first spike in response to a juxtathreshold depolarization, AP amplitude, maximal frequency, V_{Thresh} , AHP amplitude, half-width of evoked AP, Sag amplitudes in response to -40 and -100 pA). **B**, 3D plot of the unique cluster of cholinergic/GABAergic (EGFP⁺, light green) neurons obtained from the k -means algorithm. Parameters: AHP amplitude, delay of the first spike in response to juxtathreshold depolarization and maximal frequency (P2–5; $n = 23$; $N = 11$). **C**, Hierarchical clustering dendrogram for intrinsic electrophysiological properties (the same set of parameters as in **A**) of P12–15 neurons ($n = 30$; $N = 15$). **D**, 3D plot of the two clusters EGFP⁺1 (light green; $n = 18$;

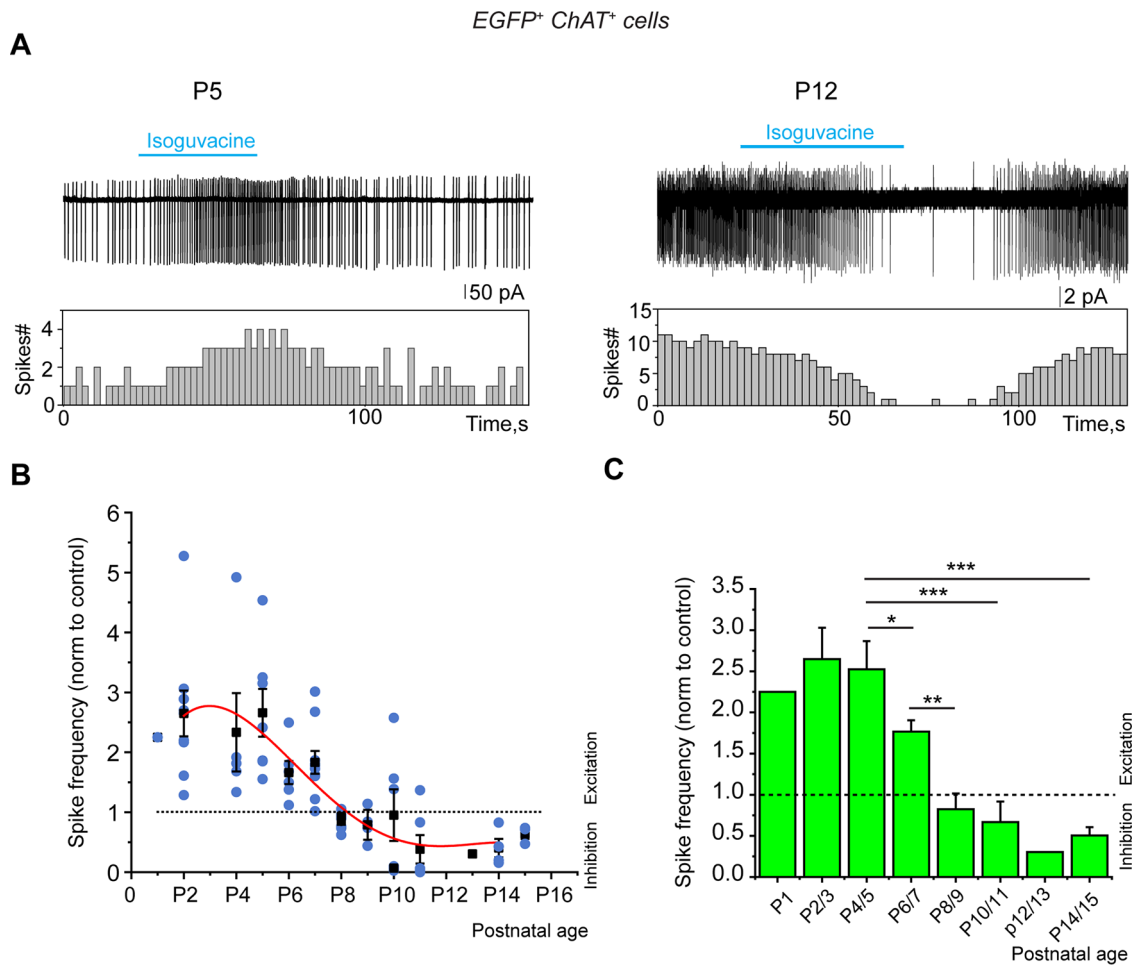


Figure 5. Developmental shift of the GABA_AR-mediated response polarity, from excitatory to inhibitory, recorded from cholinergic/GABAergic neurons (P2–15). **A**, Representative cell-attached recordings (top) and corresponding frequency histograms (bottom) of ongoing spike activity before, during, and after isoguvacine (10 μM) application at the indicated ages. **B,C**, Mean values of isoguvacine maximal effects on spike frequency [P2/3: *n* = 9 (*N* = 3); P4/5: *n* = 12 (*N* = 5); P6/7: *n* = 16 (*N* = 4); P8/9: *n* = 12 (*N* = 4); P10/11: *n* = 12 (*N* = 3); P14/15: *n* = 5 (*N* = 3)]. *n*, number of cells; *N*, number of mice. Mean ± SEM; **p* < 0.05; ***p* < 0.01; ****p* < 0.001 (Extended Data Table 5-1).

observe significant differences of their electrophysiological parameters at P14/15, despite their differences of AP and AHP amplitude at P10/11 and AP half-width at P4/5 and P10/P11 (Extended Data Fig. 3-2; Extended Data Table 3-1).

Isoguvacine application significantly decreased spike frequency at P14/15 (two times that of control; *n* = 7; *p* = 0.003; Fig. 5; Extended Data Table 5-1). GABA polarity shift occurred from P8/9 in cholinergic/GABAergic neurons since from this age isoguvacine either had no effect or significantly decreased spike frequency compared with the control. The frequency (but not the amplitude) of spontaneous GABA_AR- and AMPAR-mediated PSCs considerably increased from P4/5 to P14/15: from 2.5 ± 0.5 Hz (*n* = 9) to 13.1 ± 2.9 Hz (*n* = 9; *p* = 0.004) and from 4.2 ± 0.9 Hz (*n* = 12) to 9.2 ± 1.2 Hz, (*n* = 10; *p* = 0.004), respectively (Figs. 6, 7).

Earlier studies have suggested the presence of at least two populations of cholinergic neurons in the adult mouse forebrain (Unal et al., 2012; Laszlovszky et al., 2020). We observed a similar dichotomy at P12/15. For example, maximal frequency, AHP, and sag amplitudes were highly heterogeneous for P12/15 cholinergic/GABAergic neurons (Figs.

N = 9) and EGFP² (dark green; *n* = 12; *N* = 6) obtained from the *k*-means algorithm (P12–15). Parameters, AHP amplitude, delay of the first spike in response to juxtathreshold depolarization, and maximal frequency. Insets in **A–D** show percentage of cells belonging to each cluster. **E**, Silhouette coefficient plot for EGFP¹ and EGFP². **F–H**, Quantification of delay of the first spike in response to juxtathreshold depolarization (**F**), maximal frequency (**G**), and AHP amplitude (**H**), for datasets at P2–5 and at P12–15. *n*, number of cells, *N*, number of mice. Mean ± SEM; **p* < 0.05; ***p* < 0.01; ****p* < 0.001 (Extended Data Table 4-1). **I**, Representative responses to maximal depolarizing current pulses (black). **J**, Representative responses to the minimum current (rheobase) required to evoke an AP (red) at expanded time scale, for a P2–5 neuron and for two different P12–15 neurons belonging to the EGFP¹ or EGFP² cluster, as indicated. Cluster analysis of GABAergic and non-GABAergic cholinergic neurons (P2–5 and P12–15) based on intrinsic electrophysiological properties is presented in Extended Data Figure 4-2.

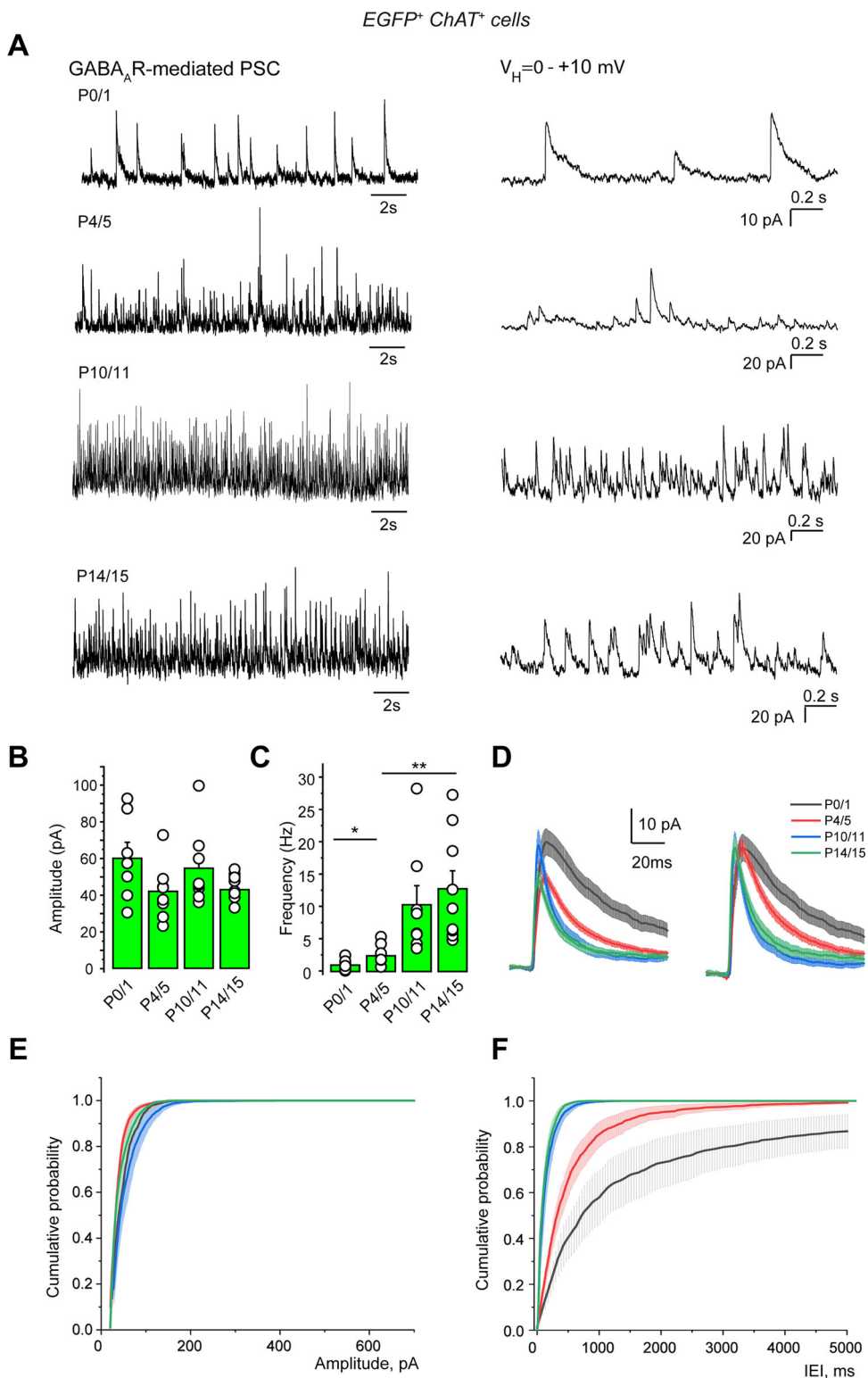


Figure 6. Development of the spontaneous GABA_AR-mediated PSC recorded from cholinergic/GABAergic neurons (P0–15). **A**, Left, Representative traces of spontaneous GABAergic PSCs (whole-cell voltage-clamp recordings, $V_H = +10$ mV) at the indicated ages. Right, Same recordings at an extended time scale. **B**, Mean amplitude. **C**, Mean frequency. **D**, Averaged traces (original on the left, normalized to the peak amplitude on the right) of spontaneous GABAergic PSCs at the same ages as in **A**. **E**, Cumulative probability of spontaneous GABAergic PSC amplitude. **F**, Cumulative probability of GABAergic PSCs interevent intervals (IEI); P0/1: $n = 7$, $N = 5$; P4/5: $n = 9$, $N = 7$; P10/11: $n = 8$, $N = 4$; P14/15: $n = 9$, $N = 6$). n , number of cells; N , number of mice. Mean \pm SEM, *: $p < 0.05$; **: $p < 0.01$; ***: $p < 0.001$ (Extended Data Fig. 6-1).

EGFP⁺ ChAT⁺ cells

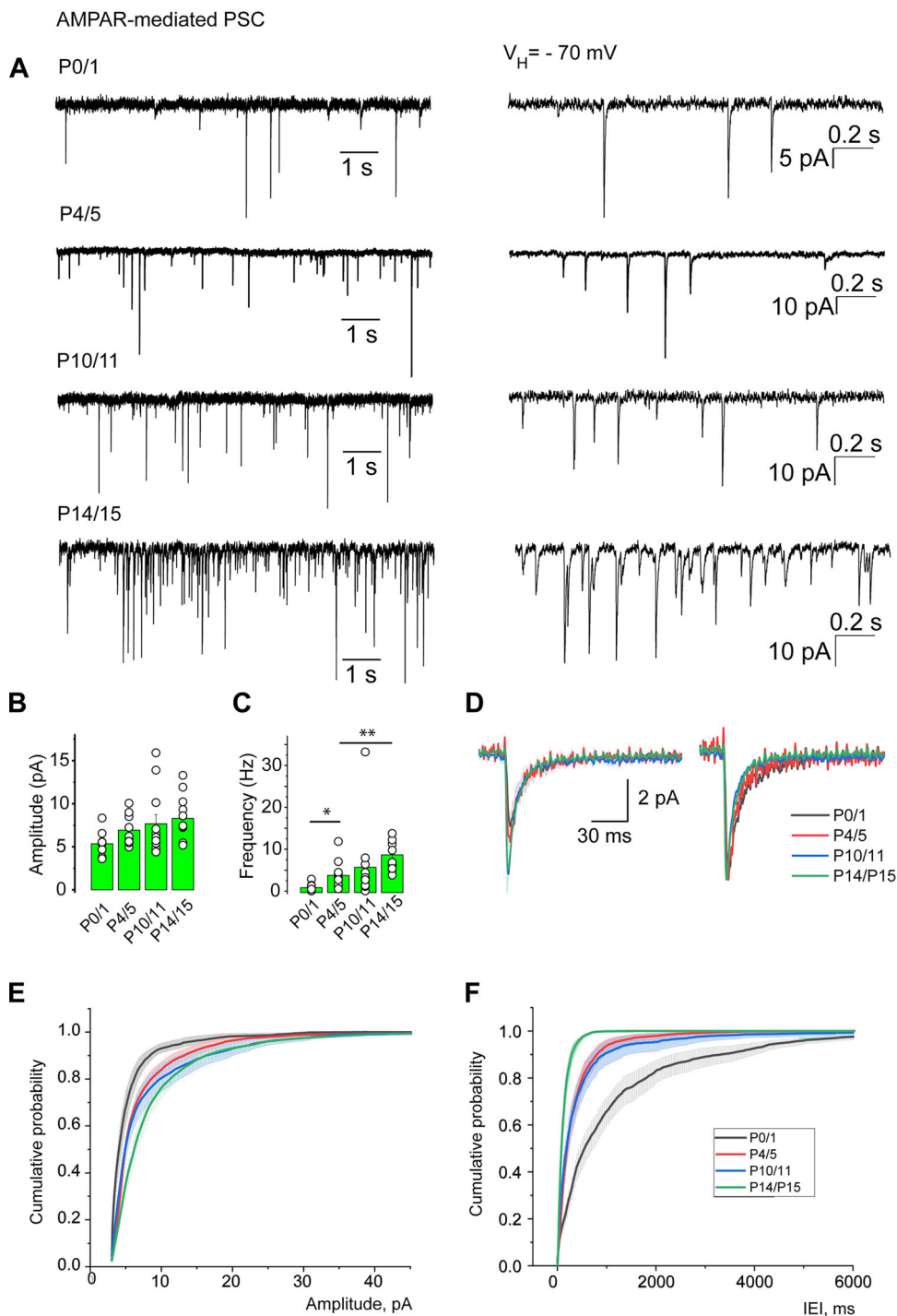


Figure 7. Development of the spontaneous AMPAR-mediated PSCs recorded from cholinergic/GABAergic neurons (P0–15). **A**, Left, Representative traces of spontaneous AMPAR-mediated PSCs (whole-cell voltage-clamp recordings, $V_H = -70$ mV) at the indicated ages. Right, Same recordings at an extended time scale. **B**, Mean amplitude. **C**, Mean frequency. **D**, Averaged traces (original on the left, normalized to the peak amplitude on the right) of spontaneous AMPAR-mediated PSCs at the same ages as in **A**. **E**, Cumulative probability of spontaneous glutamatergic PSCs amplitude. **F**, Cumulative probability of IEI. P0/1: $n = 9$, $N = 6$; P4/5: $n = 12$, $N = 6$; P10/11: $n = 12$, $N = 7$; P14/15: $n = 10$, $N = 4$. n , number of cells; N , number of mice. Mean \pm SEM. * $p < 0.05$; ** $p < 0.01$; *** $p < 0.001$ (Extended Data Fig. 7-1).

3B,E,I, 4F,G). In addition, the mean delay of the first spike in response to a juxtathreshold depolarization (rheobase) significantly increased from 239.3 ± 2.0 ms at P2/5 ($n = 25$) to 407.7 ± 48.8 ms at P12/15 ($n = 30$; $p = 0.006$). Hierarchical and k -means clustering analyses identified two groups of P12/15 cholinergic/GABAergic neurons (EGFP⁺, $n = 30$): EGFP⁺1

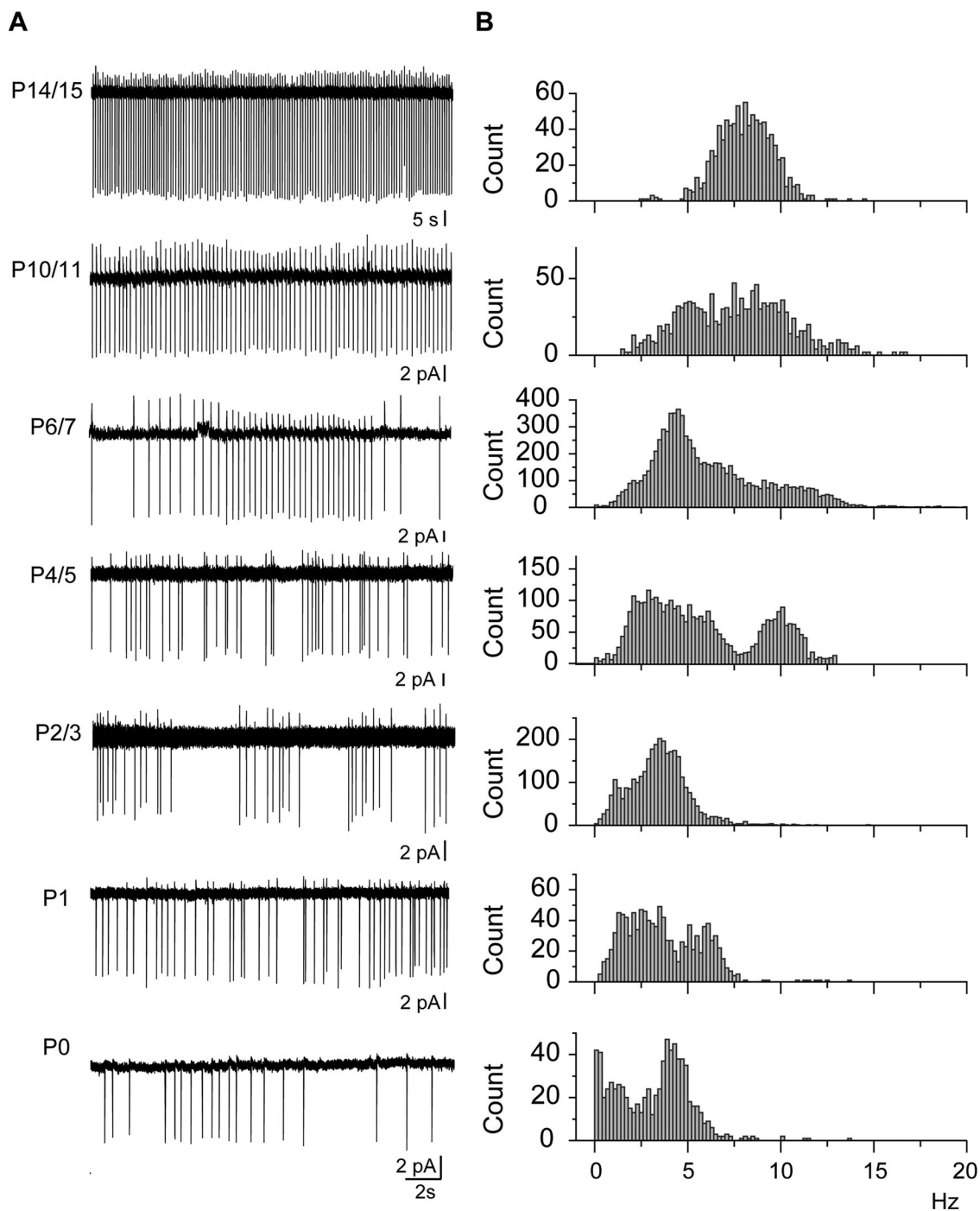


Figure 8. Patterns of ongoing activity of cholinergic/GABAergic neurons (P0–P15). **A**, Representative cell-attached recordings at the indicated ages. **B**, Pooled instantaneous frequency distributions of ongoing activities recorded as in **A**: (P0: $n = 7$, $N = 3$, 800 events; P1: $n = 6$, $N = 3$, 1,070 events; P2/3: $n = 12$, $N = 3$, 3,211 events; P4/5: $n = 8$, $N = 3$, 3,660 events; P6/7: $n = 10$, $N = 4$, 10,015 events; P10/11: $n = 10$, $N = 6$, 1,323 events; P14/15: $n = 5$, $N = 3$, 1,332 events). n , number of cells; N , number of mice.

(light green; $n = 18$; silhouette index, 0.72) and EGFP⁺2 (dark green; $n = 12$; silhouette index, 0.65; Fig. 4C–E; Extended Data Table 4-1). Comparison of electrophysiological parameters between the two populations of P12/15 cholinergic/GABAergic neurons populations (EGFP⁺1 and EGFP⁺2) revealed significant differences for delay of the first spike, maximal frequency, and AHP maximal amplitude (Fig. 4F–J; Extended Data Table 4-1). We named the EGFP⁺1 population early-firing and the EGFP⁺2 population late-firing.

Similar clustering analyses also revealed two populations of P12/15 cholinergic/non-GABAergic (EGFP⁻) neurons ($n = 18$, $N = 9$), the early-firing (EGFP⁻¹; gray; $n = 14$; silhouette index, 0.68) and late-firing (EGFP⁻²; black; $n = 4$; silhouette index = 0.64) populations (Extended Data Fig. 4-2C–E). We did not observe significant differences between parameters tested (maximal frequency of evoked spikes, delay of the first spike in response to juxtathreshold depolarization, and AHP maximal amplitude) between EGFP⁺¹ versus EGFP⁻¹ and EGFP⁺² versus EGFP⁻² (Extended Data Fig. 4-2D,F–J; Extended Data Table 4-1).

Collectively, these results show that the major changes in dendritic trees and membrane parameters of all cholinergic neurons principally occurred during the first postnatal week. Extrinsic parameters such as afferent connections activity was present from P0 and considerably increased during the second postnatal week. They also highlight the low impact of GABAergic cotransmission on the development and types of functional cholinergic populations. After the first postnatal week, in parallel to GABA polarity shift, with the increase of active glutamatergic and GABAergic connections and the regularization of spontaneous in vitro activity, cholinergic GABAergic or non-GABAergic neurons separate into two distinct populations according to intrinsic electrophysiological parameters. The new population, the late-firing neurons, represented 40% of the P12/15 cholinergic neurons. They were less excitable than early-firing neurons since they responded with a longer delay to juxtathreshold depolarizations and with a lower maximal frequency to large depolarizations (Fig. 4F,G,I,J; Extended Data Fig. 4-2F,G,I,J). They also displayed a large AHP maximal amplitude (Fig. 4H; Extended Data Fig. 4-2H). These two populations corresponded to the two populations previously described in adult rodents in vitro and in vivo (Unal et al., 2012; Laszlovsky et al., 2020).

Discussion

From perinatal days up to the end of the first postnatal week, when GABA_AR current polarity shift has not yet occurred, SI/NBM cholinergic neurons, whether they have coexpressed or still express GABAergic markers, belong to a single homogenous population of developing, spontaneously active, bursting, and early-firing neurons, connected to and depolarized by both their glutamatergic and GABAergic afferents. At that stage, during the first postnatal days, the only heterogeneity of SI/NBM cholinergic neurons concerned their ability to corelease GABA. During these early postnatal days, between P2/3 and P8/9, the significant decrease in some of the morphological parameters of SI/NBM cholinergic neurons (area under the Sholl curve, total dendritic length, critical value, and number of dendritic nodes) probably reflects dendrite pruning. This process of dendrite elimination that initially forms in abundance occurs during the early stages of normal development of neuronal networks. It is essential to sculpt the mature nervous system of both vertebrates and invertebrates (Konur and Ghosh, 2005).

The excitatory effect of the GABA_AR agonist isoguvacine until P8/9 suggests that GABA_AR-mediated transmission is depolarizing and excitatory during the first postnatal week. Bath applied isoguvacine could, however, have an indirect excitatory effect on SI/NBM neurons at P5 via the release of glutamate by glial cells (excited by isoguvacine) or via the inhibition of excitatory interneurons (disinhibition). But glia is much less developed in very young brains than later. Although the developmental shift in GABA action has been widely demonstrated in vitro (for review, see Ben Ari et al., 2007), results in vivo in anaesthetized animals (Kirmse et al., 2015) have challenged this finding. But experiments carried out in nonanesthetized pups (Murata and Colonnese, 2020) showed a clear excitatory effect of GABA interneurons in vivo in young rodents. Persistent shift of GABA polarity from depolarizing to hyperpolarizing mode is due to the reduction in the intracellular chloride concentration and is a critical event for early brain circuits' development and their orchestrated activity-dependent formation.

SI/NBM cholinergic neurons generated AMPAR-mediated and GABA_AR-mediated spontaneous currents already at birth, with a frequency which increased during the first postnatal week. These inputs may originate, as in the adult, from locally arborizing glutamatergic and GABAergic neurons which form complex networks with cholinergic neurons (Zaborszky and Duque, 2000; Gritti et al., 2006; McKenna et al., 2021). Double immunolabeling for ChAT and the vesicular glutamate transporters (Vglut) in the adult rat SI showed synapses between Vglut1 or Vglut2 boutons and cholinergic dendrites and occasionally between Vglut2 boutons and cholinergic cell bodies (Hur et al., 2009). Glutamatergic inputs can also arise from cortical areas since the anterograde transport of *Phaseolus vulgaris* leucoagglutinin (PHA-L) combined with AChE histochemistry or ChAT immunocytochemistry revealed rich PHA-L-labeled projections to discrete parts of the BF cholinergic system essentially originating from all adult prefrontal areas investigated (Gaykema et al., 1991).

GABA_AR-mediated spontaneous currents were present at birth and then increased in frequency. Afferent GABAergic terminals were likely to arise from both local and extrinsic afferent sources. BF GABAergic cells are about twice as numerous as BF cholinergic cells (Gritti et al., 1993). GABAergic (GAD⁺) varicosities were identified in the immediate vicinity of biocytin-filled soma and dendrites of electrophysiologically identified cholinergic cells in the adult guinea pig NBM (Khateb et al., 1998) and GABAergic axons synapse onto adult rat cholinergic neurons (Zaborszky et al., 1986). Amygdala, striatum, and accumbens also send GABAergic projections to adult BF cholinergic neurons (Zaborszky et al., 1986; Zaborszky and Cullinan, 1992; Paré and Smith, 1994; Gielow and Zaborszky, 2017). GABA_AR-mediated spontaneous PSCs were excitatory until the end of the first postnatal week.

Interestingly, P0/5 SI/NBM cholinergic neurons received glutamatergic and GABAergic inputs which were both excitatory, and they responded with a short delay to juxta- and suprathreshold depolarizations. This, combined to a high

membrane resistance, a small amplitude AHP, and a large sag suggesting the presence of a pacemaker H current, allowed P0/P5 cholinergic neurons to spontaneously fire. Moreover, P0/P5 cholinergic neurons tended to spontaneously burst. This bursting activity is likely to propagate to the cortex where cholinergic terminals are already present. All these characteristics strongly suggest that during the first postnatal days, SI/NBM cholinergic neurons can spontaneously release ACh or ACh and GABA in the developing cortical layers allowing them to fulfill their role in cortical development during the first postnatal days. Coreleased GABA, which is probably depolarizing/excitatory to cortical cells during early postnatal days, should also play a role in cortical development (Represa and Ben-Ari, 2005).

During the second postnatal week, a second population of SI/NBM cholinergic neurons appeared, the late-firing neurons, which fired with a longer delay in response to subthreshold depolarizations, displaying a lower maximal frequency due to a large-amplitude AHP. The same two cholinergic populations have been described in the adult rodent BF, *in vitro* and *in vivo* (Unal et al., 2012; Laszlovszky et al., 2020). We show here that the classification of SI/NBM cholinergic neurons in early or late-firing populations was uncorrelated to the coexpression of GABA release markers (Kosaka et al., 1988; Tkatch et al., 1998; Saunders et al., 2015; Granger et al., 2016).

The two electrophysiologically identifiable types of BF cholinergic neurons, the early- and late-firing neurons, may fulfill different functions in the adult *in vivo* (Laszlovszky et al., 2020). The *in vivo* BF_{BURST} (bursting firing) neurons (70%), corresponding to the *in vitro* early-firing neurons, generated bursts with a strong synchrony with each other and auditory cortical oscillations, preferentially after behavioral reinforcement, water reward, or air-puff punishment, suggesting that they may have a strong impact on cortical processing. In contrast, the *in vivo* BF_{REG} (regular firing) neurons (30%), corresponding to the *in vitro* late-firing neurons, were nonbursting neurons with shorter spikes and a bigger AHP. Coupling between regular firing neurons and the auditory cortical neurons was strongest before mice made successful hits, thus predicting behavioral performance. The proportion of each subpopulation varied between anterior and posterior BF. As the anterior and posterior BF have different projection targets (Rye et al., 1984; Unal et al., 2012), distinct brain regions receive different proportions of bursting cholinergic input.

The functional diversity of BF cholinergic neurons may result from the multiplicity of embryonic origins (medial ganglionic eminence, preoptic area, septal neuroepithelium; Magno et al., 2017), ventral area of the pallial telencephalon (pallium; Pombero et al., 2011), and/or combinatorial gene expression including a number of transcription factors during early developmental stages (see review in Allaway and Machold, 2017; Ahmed et al., 2019) and/or from their birth date (Allaway et al., 2020). The expression or not of GABA corelease markers is the only functional diversity present in the perinatal period. Between P0 and P7, all SI/NBM cholinergic neurons have properties (highly excitable, excited by both glutamatergic and GABAergic afferents) that give them the capacity to provide ACh or ACh and GABA to the developing cortex. It is only during the second postnatal week, in parallel to GABA polarity shift, that two functional populations of SI/NBM cholinergic neurons are present and fulfill two different roles in cortical processing. The present characterization of the early postnatal activity of basal cholinergic neurons allows understanding the crucial role of ACh in the early development of cortical networks. Furthermore, the transition of NB/SI cholinergic neurons from a single population of early responding neurons, activated by both GABA and glutamate during the postnatal period, to two populations of neurons with more complex properties from P15 onward is an example of how neurons in a structure shift from a developmental role to a functional role.

Conclusion

We propose that the early development of a single and homogeneous population of highly excitable SI/NBM cholinergic neurons (GABAergic or not), together with their activation by both their glutamatergic and GABAergic afferents, allows the release of ACh and GABA in the developing sensorimotor cortical layers already during the first postnatal week (Gaykema et al., 1991; Saunders et al., 2015; Zaborszky et al., 2015; Granger et al., 2016; Gielow and Zaborszky, 2017). This would explain their early determinant role in the development of cortical neurons and networks (Hohmann and Berger-Sweeney, 1998). During the second postnatal week, in parallel with the GABA polarity shift, SI/NBM cholinergic neurons differentiate into two distinct populations that exert different functional roles in adults (Laszlovszky et al., 2020).

References

- Ahmed NY, Knowles R, Dehorter N (2019) New insights into cholinergic neuron diversity. *Front Mol Neurosci* 12:204.
- Allaway KC, Machold R (2017) Developmental specification of forebrain cholinergic neurons. *Dev Biol* 421:1–7.
- Allaway KC, Muñoz W, Tremblay R, Sherer M, Herron J, Rudy B, Machold R, Fishell G (2020) Cellular birthdate predicts laminar and regional cholinergic projection topography in the forebrain. *Elife* 9:e63249.
- Atluri P, Fleck MW, Shen Q, Mah SJ, Stadfeld D, Barnes W, Goderie SK, Temple S, Schneider AS (2001) Functional nicotinic acetylcholine receptor expression in stem and progenitor cells of the early embryonic mouse cerebral cortex. *Dev Biol* 240:143–156.
- Ballinger EC, Ananth M, Talmage DA, Role LW (2016) Basal forebrain cholinergic circuits and signaling in cognition and cognitive decline. *Neuron* 91:1199–1218.
- Ben Ari Y, Gaiarsa JL, Tyzio R, Khazipov R (2007) GABA: a pioneer transmitter that excites immature neurons and generates primitive oscillations. *Physiol Rev* 87:1215–1284.
- Berger-Sweeney J, Stearns NA, Murg SL, Floerke-Nashner LR, Lappi DA, Baxter MG (2001) Selective immunolesions of cholinergic

- neurons in mice: effects on neuroanatomy, neurochemistry, and behavior. *J Neurosci* 21:8164.
- Boskovic Z, Meier S, Wang Y, Milne MR, Onraet T, Tedoldi A, Coulson EJ (2019) Regulation of cholinergic basal forebrain development, connectivity, and function by neurotrophin receptors. *Neuronal Signal* 3:NS20180066.
- Branchereau P, Cattaert D, Delpy A, Allain AE, Martin E, Meyrand P (2016) Depolarizing GABA/glycine synaptic events switch from excitation to inhibition during frequency increases. *Sci Rep* 6:21753.
- Brown RE, Basheer R, McKenna JT, Strecker RE, McCarley RW (2012) Control of sleep and wakefulness. *Physiol Rev* 92:1087–1187.
- Bruel-Jungerman E, Lucassen PJ, Francis F (2011) Cholinergic influences on cortical development and adult neurogenesis. *Behav Brain Res* 221:379–388.
- Case DT, Burton SD, Gedeon JY, Williams SPG, Urban NN, Seal RP (2017) Layer- and cell type-selective co-transmission by a basal forebrain cholinergic projection to the olfactory bulb. *Nat Commun* 8:652.
- Claridge-Chang A, Assam PN (2016) Estimation statistics should replace significance testing. *Nat Methods* 13:108–109.
- Demsar J, et al. (2014) Orange: data mining toolbox in python. *J Mach Learn Res* 14:2349–2353.
- Gaykema RPA, Van Weeghel R, Hersh LB, Luiten PGM (1991) Prefrontal cortical projections to the cholinergic neurons in the basal forebrain. *J Comp Neurol* 303:563–583.
- Gielow MR, Zaborszky L (2017) The input-output relationship of the cholinergic basal forebrain. *Cell Rep* 18:1817–1830.
- Granger AJ, Mulder N, Saunders A, Sabatini BL (2016) Cotransmission of acetylcholine and GABA. *Neuropharmacology* 100:40–46.
- Grill WM, Snyder AN, Miocinovic S (2004) Deep brain stimulation creates an informational lesion of the stimulated nucleus. *Neuroreport* 15:1137–1140.
- Gritti I, Henny P, Galloni F, Mainville L, Mariotti M, Jones BE (2006) Stereological estimates of the basal forebrain cell population in the rat, including neurons containing choline acetyltransferase (chat), glutamic acid decarboxylase (GAD) or phosphate-activated glutaminase (PAG) and colocalizing vesicular glutamate transporters (VGLUTs). *Neuroscience* 143:1051.
- Gritti I, Mainville L, Jones BE (1993) Codistribution of GABA- with acetylcholine-synthesizing neurons in the basal forebrain of the rat. *J Comp Neurol* 329:438–457.
- Henny P, Jones BE (2008) Projections from basal forebrain to prefrontal cortex comprise cholinergic, GABAergic and glutamatergic inputs to pyramidal cells or interneurons. *Eur J Neurosci* 27:654–670.
- Ho J, Tumkaya T, Aryal S, Choi H, Claridge-Chang A (2019) Moving beyond P values: data analysis with estimation graphics. *Nat Methods* 16:565–566.
- Hohmann CF (2003) A morphogenetic role for acetylcholine in mouse cerebral neocortex. *Neurosci Biobehav Rev* 27:351–363.
- Hohmann CF, Berger-Sweeney J (1998) Cholinergic regulation of cortical development and plasticity. New twists to an old story. *Perspect Dev Neurobiol* 5:401–425.
- Hohmann CF, Brooks AR, Coyle JT (1988) Neonatal lesions of the basal forebrain cholinergic neurons result in abnormal cortical development. *Brain Res* 470:253–264.
- Höhmann CF, Ebner FF (1985) Development of cholinergic markers in mouse forebrain. I. Choline acetyltransferase enzyme activity and acetylcholinesterase histochemistry. *Dev Brain Res* 23:225–241.
- Hur EE, Edwards RH, Rommer E, Zaborszky L (2009) Vesicular glutamate transporter 1 and vesicular glutamate transporter 2 synapses on cholinergic neurons in the sublentiform gray of the rat basal forebrain: a double-label electron microscopic study. *Neuroscience* 164:1721–1731.
- Khateb A, Fort P, Williams S, Serafin M, Mühlethaler M, Jones BE (1998) GABAergic input to cholinergic nucleus basalis neurons. *Neuroscience* 86:937–947.
- Kirmse K, Kummer M, Kovalchuk Y, Witte OW, Garaschuk O, Holthoff K (2015) GABA depolarizes immature neurons and inhibits network activity in the neonatal neocortex in vivo. *Nat Commun* 6:7750.
- Konur S, Ghosh A (2005) Calcium signaling and the control of dendritic development. *Neuron* 46:401–405.
- Kosaka T, Tauchi M, Dahl JL (1988) Cholinergic neurons containing GABA-like and/or glutamic acid decarboxylase-like immunoreactivities in various brain regions of the rat. *Exp Brain Res* 70:605–617.
- Kuczewski N, Aztiria E, Leanza G, Domenici L (2005) Selective cholinergic immunolesion affects synaptic plasticity in developing visual cortex. *Eur J Neurosci* 21:1807–1814.
- Laszlovszky T, Schlingloff D, Hegedüs P, Freund TF, Gulyás A, Kepecs A, Hangya B (2020) Distinct synchronization, cortical coupling and behavioral function of two basal forebrain cholinergic neuron types. *Nat Neurosci* 23:992–1003.
- Lozovaya N, et al. (2018) GABAergic inhibition in dual-transmission cholinergic and GABAergic striatal interneurons is abolished in Parkinson disease. *Nat Commun* 9:1422.
- Magno L, Barry C, Schmidt-Hieber C, Theodotou P, Häusser M, Kessaris N (2017) NKX2-1 is required in the embryonic septum for cholinergic system development, learning, and memory. *Cell Rep* 20:1572–1584.
- McKenna JT, et al. (2021) Characterization of basal forebrain glutamate neurons suggests a role in control of arousal and avoidance behavior. *Brain Struct Funct* 226:1755.
- Mechawar N, Descarries L (2001) The cholinergic innervation develops early and rapidly in the rat cerebral cortex: a quantitative immunocytochemical study. *Neuroscience* 108:555–567.
- Mesulam MM, Mufson EJ, Wainer BH, Levey AI (1983) Central cholinergic pathways in the rat: an overview based on an alternative nomenclature (Ch1-Ch6). *Neuroscience* 10:1185–1201.
- Monosov IE, Leopold DA, Hikosaka O (2015) Neurons in the primate medial basal forebrain signal combined information about reward uncertainty, value, and punishment anticipation. *J Neurosci* 35:7443.
- Murata Y, Colonnese MT (2020) GABAergic interneurons excite neonatal hippocampus in vivo. *Sci Adv* 6:eaba1430.
- Paré D, Smith Y (1994) GABAergic projection from the intercalated cell masses of the amygdala to the basal forebrain in cats. *J Comp Neurol* 344:33–49.
- Pombero A, Bueno C, Saglietti L, Rodenas M, Guimera J, Bulfone A, Martinez S (2011) Pallial origin of basal forebrain cholinergic neurons in the nucleus basalis of Meynert and horizontal limb of the diagonal band nucleus. *Development* 138:4315–4326.
- Represa A, Ben-Ari Y (2005) Trophic actions of GABA on neuronal development. *Trends Neurosci* 28:278–283.
- Ricceri L, Hohmann C, Berger-Sweeney J (2002) Early neonatal 192 IgG saporin induces learning impairments and disrupts cortical morphogenesis in rats. *Brain Res* 954:160–172.
- Robertson RT, et al. (1998) Neonatal treatment with 192 IgG-saporin produces long-term forebrain cholinergic deficits and reduces dendritic branching and spine density of neocortical pyramidal neurons. *Cereb Cortex* 8:142–155.
- Rye DB, Wainer BH, Mesulam MM, Mufson EJ, Saper CB (1984) Cortical projections arising from the basal forebrain: a study of cholinergic and noncholinergic components employing combined retrograde tracing and immunohistochemical localization of choline acetyltransferase. *Neuroscience* 13:627–643.
- Saunders A, Granger AJ, Sabatini BL (2015) Corelease of acetylcholine and GABA from cholinergic forebrain neurons. *Elife* 2015:e06412.
- Tkatch T, Baranauskas G, Surmeier DJ (1998) Basal forebrain neurons adjacent to the globus pallidus co-express GABAergic and cholinergic marker mRNAs. *Neuroreport* 9:1935–1939.
- Unal CT, Golowasch JP, Zaborszky L (2012) Adult mouse basal forebrain harbors two distinct cholinergic populations defined by their electrophysiology. *Front Behav Neurosci* 6:21.
- Wu H, Williams J, Nathans J (2014) Complete morphologies of basal forebrain cholinergic neurons in the mouse. *Elife* 2014:1–17.

- Záborsky L, Cullinan WE (1992) Projections from the nucleus accumbens to cholinergic neurons of the ventral pallidum: a correlated light and electron microscopic double-immunolabeling study in rat. *Brain Res* 570:92–101.
- Záborsky L, Csordas A, Mosca K, Kim J, Gielow MR, Vadasz C, Nadasdy Z (2015) Neurons in the basal forebrain project to the cortex in a complex topographic organization that reflects corticocortical connectivity patterns: an experimental study based on retrograde tracing and 3D reconstruction. *Cereb Cortex* 25:118–137.
- Zaborszky L, Duque A (2000) Local synaptic connections of basal forebrain neurons. *Behav Brain Res* 115:143–158.
- Záborsky L, Heimer L, Eckenstein F, Leranth C (1986) GABAergic input to cholinergic forebrain neurons: an ultrastructural study using retrograde tracing of HRP and double immunolabeling. *J Comp Neurol* 250:282–295.
- Zant JC, et al. (2016) Cholinergic neurons in the basal forebrain promote wakefulness by actions on neighboring non-cholinergic neurons: an opto-dialysis study. *J Neurosci* 36:2057–2067.